Laser and Particle Beams (2015), *33*, 143–149.

doi:10.1017/S0263034615000026

Influence of target curvature on ion acceleration in radiation pressure acceleration regime

DEEPAK DAHIYA,[1] ASHOK KUMAR,[2] AND V. K. TRIPATHI[1]

[1]Physics Department, IIT Delhi, New Delhi, India
[2]Physics Department, AIAS, Amity University, Noida, India

(RECEIVED 2 April 2014; ACCEPTED 6 January 2015)

Abstract

Ion acceleration from submicron thick foil target irradiated by a circularly polarized laser is studied using multidimensional particle-in-cell simulations. Convex, flat, and concave target shapes are considered. Radius of curvature of curved target is of the order of laser width in transverse direction. Accelerated ion beam of highest peak energy and least energy spread is obtained from concave target, whereas total accelerated charge is highest in convex target. It is attributed to the change in the growth of transverse instabilities and geometrical effects due to target curvature in initial stages of acceleration process. The variation in the radius of curvature of the foil depends on the ratio of initial spot size to the radius of curvature. Faster reduction in curvature is achieved for tightly focused Gaussian pulses as conjectured by the model.

Keywords: Laser driven ion acceleration; radiation pressure acceleration; Target curvature

1. INTRODUCTION

The acceleration of energetic ions by interaction of intense short laser pulse with solid thin foil target is an area of great interest (Macchi *et al.*, 2013) and importance having potential applications such as, producing high-energy-density matter (Patel, 2003; Borghesi, 2004), radio graphing transient processes (Borghesi *et al.*, 2002), tumor therapy (Bulanov *et al.*, 2002; Fourkal *et al.*, 2007), generating isotopes in positron emission tomography (Spencer *et al.*, 2001), material modification (Trtica *et al.*, 2013; Ahmad *et al.*, 2014; Akram *et al.*, 2014), X-ray generation (Kumar *et al.*, 2014), and fast ignition of fusion cores (Temporal *et al.*, 2009; Roth, 2001). Ion beams with energies up to several tens of MeV has been obtained in experiments and mechanism is generally attributed to target normal sheath acceleration (TNSA) (Clark, 2000; Psikal *et al.*, 2008; Bin, 2009; Macchi *et al.*, 2009; Brady & Arber, 2011). However, these beams have low particle density and high-energy spread. Several schemes for enhanced interaction of ultrashort laser pulses with plasmas are being pursued worldwide to understand the physics of the process and its effects on the ion acceleration mechanisms (Lee *et al.*, 2004; Bagchi *et al.*, 2008; Shoucri *et al.*, 2008; Andreev *et al.*, 2009; Regam, 2011; Jablonski *et al.*, 2014).

Recent theories and simulation studies have focused on the use of circularly polarized (CP) laser pulses to accelerate high-density ion bunches at the front surface of thin foils (Macchi *et al.*, 2005; Hegelich *et al.*, 2006; Chen *et al.*, 2008; Eliasson *et al.*, 2009; Robinson *et al.*, 2009; Yan *et al.*, 2009; Tripathi *et al.*, 2009; Kim *et al.*, 2013). For CP pulses, the ponderomotive force has no oscillating component; hence, electrons are steadily pushed forward inducing a charge separation field which can accelerate ions. The absence of hot electrons circulating through the target suppresses rapid foil decompression and allows radiation pressure acceleration (RPA) to dominate at more moderate intensities. Yan *et al.* (2009) in simulations and Tripathi *et al.* (2009) theoretically, presented a novel scheme for producing mono energetic protons, in hundreds of MeV range, with a specific foil thickness, equal to the distance of maximum charge separation at which the space charge force on electrons is balanced by the ponderomotive force. Nearly all the electrons of the foil are swept by ponderomotive force and piled up at the rear surface of the foil. Ions are detached from the surface by the combined repulsive electric force and the laser ponderomotive force, into vacuum to form a moving double layer, trapping the ions in the sheath of width $/\omega_p$, the skin depth. Qiao *et al.* (2009) suggested that the acceleration process is composed of two connected

Address correspondence and reprint requests to: Ashok Kumar, Physics Department, AIAS, Amity University, Noida, Noida-201303, U. P., India. E-mail: akumar16@amity.edu

stages: Relativistic "hole boring" (Gibbon, 2005; Macchi *et al.*, 2005) and "light sail" (Robinson *et al.*, 2009) RPA. They found that the stability of acceleration process depends critically on a smooth transition between two stages. Jain *et al.* (2013) have numerically studied the interaction of ultrashort pulses with relativistic mirrors and conjectured the generation of intense X rays and γ rays. Many studies in the TNSA regime have reported that target curvatures can affect the hot electron generation in laser–solid interactions (Clark, 2000; Psikal *et al.*, 2008; Bin, 2009). Psikal *et al.* (2008) found that the proton energy can be increased using a cylindrical target in TNSA. The increase is attributed to an enhancement of light absorption by the curved front surface of the target. Curvature can also affect the hot electron transport inside the target. Bin (2009) studied the effect of front-surface curvature on TNSA protons using two-dimensional (2D) particle-in-cell (PIC) simulations, and found that the highest energy protons were from the concave target. Furthermore in the RPA regime, when solid thin foil of sub-micron thickness is irradiated by Gaussian laser pulses, the foil gets curved due to non-uniform laser intensity in transverse dimension. PIC simulations results indicate that Rayleigh–Taylor or Weibel-like transverse instabilities grows as foil changes shape (Silva *et al.*, 2002; Pegoraro & Bulanov, 2007; Robinson *et al.*, 2009; Palmer *et al.*, 2012). These factors increase the energy spread and limit the higher energy gain. Sentoku *et al.* (2004) have performed 3D PIC simulations to study short pulse interaction with conical targets and conjectured efficient energy transfer to the target electrons.

In this paper, we restudy the ion acceleration scheme in the RPA regime by considering concave and convex curvatures in thin foil targets. Comparisons are made with the flat foil target proposed in the earlier studies (Qiao *et al.*, 2009; Tripathi *et al.*, 2009; Yan *et al.*, 2009). Concave and convex foil targets have radius of curvature of the order of laser spot size. The growth of transverse instabilities, during changing shape phase, is least in the concave target; this results in highest peak energy and least energy spread. In Section 2, we develop a theoretical estimate for the variation in the curvature of the foil with different spot size of the pulse. In Section 3, the results of the corresponding PIC simulations are presented. In Section 4, the numerical and simulation results are analyzed and discussed.

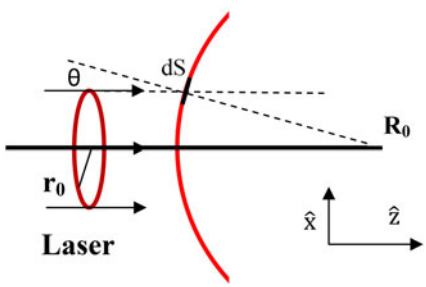

Fig. 1. The Gaussian laser pulse with spot size (r_0) impinges on the convex foil with radius of curvature (R_0). Laser makes an angle θ with length element *ds*.

2. THEORETICAL ANALYSIS

Let us consider a curved foil of uniform thickness (l) given by the equation

$$z(t) = z_0(t) + \frac{x^2}{2R(t)}, \tag{1}$$

where $R(t)$ is the radius of curvature as a function of time, $z_0(t)$ is the location of the center of axis at $t = 0$ (cf. Fig. 1). Defining $G \equiv 1/R$, Eq. (1) can be rewritten as

$$z(t) = z_0(t) + G(t)\frac{x^2}{2}. \tag{2}$$

The laser intensity profile impinged on the foil from left is

$$I = I_0\, e^{-x^2/r_0^2}, \tag{3}$$

where r_0 is the laser spot size. The force exerted by the laser on a segment of the foil of length *ds* is given by

$$\frac{2I}{c}\cos^2\theta\, ds, \tag{4}$$

where θ is the angle laser makes with the normal to the segment, and

$$\cos^2\theta = [1 + (dz/dx)^2]^{-1} \approx 1 - x^2/R^2. \tag{5}$$

The equation of motion of the foil segment *ds* (in the *x*–*z* plane) and γ the width unity can be written as

$$m_i\, n_0\, l\frac{d^2z}{dt^2} = \frac{2I}{c}\cos^2\theta, \tag{6}$$

where m_i is the mass of ions.

$$\frac{d^2z}{dt^2} = g_0 e^{-x^2/r_0^2}\ \cos^2\theta, \tag{7}$$

where $g_0 \equiv (2\ I_0)/(c\ m_i\ n_0\ l)$. Using Eq. (5), the above equation can be expressed as

$$\frac{d^2z}{dt^2} = g_0\left(1 - \frac{x^2}{r_0^2}\right)\left(1 - \frac{x^2}{R^2}\right), \tag{8}$$

Using Eq. (2) and equating different powers of x on both sides one gets

$$\frac{d^2G}{dt^2} = -2\ g_0\left[\frac{1}{r_0^2} + G^2\right], \tag{9}$$

$$\frac{d^2z_0}{dt^2} = g_0\ , \tag{10}$$

https://doi.org/10.1017/S0263034615000026 Published online by Cambridge University Press

and

$$z_0 = g_0 t^2/2. \tag{11}$$

By replacing $\partial^2/\partial t^2$ by $\left[2\, g_0 \left\{ z_0 \frac{\partial^2}{\partial z_0^2} + \frac{1}{2}\frac{\partial}{\partial z_0} \right\}\right]$ and defining the radius of curvature as $\Psi(\equiv r_0 G)$ and the normalized distance of propagation of the center of the foil as $\xi(\equiv z_0/r_0)$, one can rewrite Eq. (9)
as

$$\xi \frac{\partial^2 \Psi}{\partial \xi^2} + \frac{1}{2}\frac{\partial \Psi}{\partial \xi} = -2 - \Psi^2. \tag{12}$$

3. PIC SIMULATION

We carried out 2D simulations using fully relativistic PIC code VORPAL (Nieter & Cary, 2004). A high-power CP Gaussian laser pulse strikes a thin foil of the highly overdense plasma. Required laser intensity and optimum target thickness for stable and sustained acceleration in the RPA regime, are calculated according to the schemes described in recent studies (Qiao *et al.*, 2009; Tripathi *et al.*, 2009). Laser intensity required to produce relativistic ions in the hole-boring stage is [Eq. (3). of Qiao *et al.* (2009)].

$$\frac{I_0}{m_i n_i c^3} \approx \frac{1}{4}. \tag{13}$$

For protons ($m_i/m_e = 1836$), the intensity is $I_0(n_0/n_e) \times 10^{20} \times (1\ \mu\text{m}/\lambda)^2$ W cm^{-2}, where n_0 is the initial foil density, λ is the laser wavelength in microns, $n_c = m_e\ \omega^2/4\pi e^2$ is the critical density with e and m_e the electron charge and mass, respectively and ω is the laser frequency. Such intensities are large enough to achieve a smooth transition between "hole boring" and "light sail" stages. Target thickness required to prevent blow out of all electrons in foil by laser ponderomotive force, is estimated by condition that maximum charge separation field $E_{\parallel,\max} = 4\ \pi\ e\ n_0\ l_0$ should be larger than the ponderomotive force ($v \times B_L$). This gives the condition [Eq. (4). of Qiao *et al.* (2009)]

$$\frac{l_0}{\lambda} \gtrsim \frac{1}{2\pi} \sqrt{\frac{n_c m_i}{n_i m_e}} \sqrt{\frac{I}{m_i n_i c^3}}. \tag{14}$$

Choosing $l = l_0$ and $n_i = n_0$, the foil thickness should satisfy $l_0 \gtrsim 3.41\ \sqrt{n_c/n_0}\ \lambda$.

In our simulations, a CP laser pulse, Gaussian in space and time, having peak intensity 6.3×10^{22} W cm^{-2}, wavelength 1 μm, spot size 16 μm (full width at half maximum) and duration 250 fs, is launched from the left boundary. Laser strikes an overdense plasma foil normally. The total simulation box is $60 \times 50\ \mu\text{m}^2$ having 6000×5000 cells in the (z, x) plane. Each cell is filled with 100 macroparticles per species. The foil plasma consists of two species: Electrons and protons, both having equal density $n = n_e = n_i = 100\ n_c$, where $n_c = 1.1 \times 10^{21}$ cm^3 is the critical density. Thickness of foil is 0.35 μm [from Eq. (14)]. Radius of curvature of concave and convex foil targets is 50 μm. The boundary conditions are absorbing for both electromagnetic waves and macro particles.

4. RESULTS AND DISCUSSION

We start with the flat target case, Figure 2 plots ion density n_i/n_c at (a) 10, (b) 44, (c) 60, (d) 74, (e) 90, (f) 160, and (g) 230 fs. Figure 2a shows the foil target of 100 n_c density and 0.35 μm thickness just before the laser pulse strikes the target. Figure 2b corresponds to hole-boring stage, two layers starts to appear: Highly dense green layer on the back side of the target and lower density protons left as red layer. The flat foil changes shape due to non-uniform laser push in the transverse direction and the resulting curved foil is shown in Figure 2c. Transverse bunching of protons grows as the change in the shape of foil continues in Fig. 2d. The foil attains its maximum curvature and looks like a concave foil in Figure 2e. As the foil is moving with relativistic velocity, and the growth rate of transverse instabilities depends inversely on the relativistic factor, the foil stays intact and

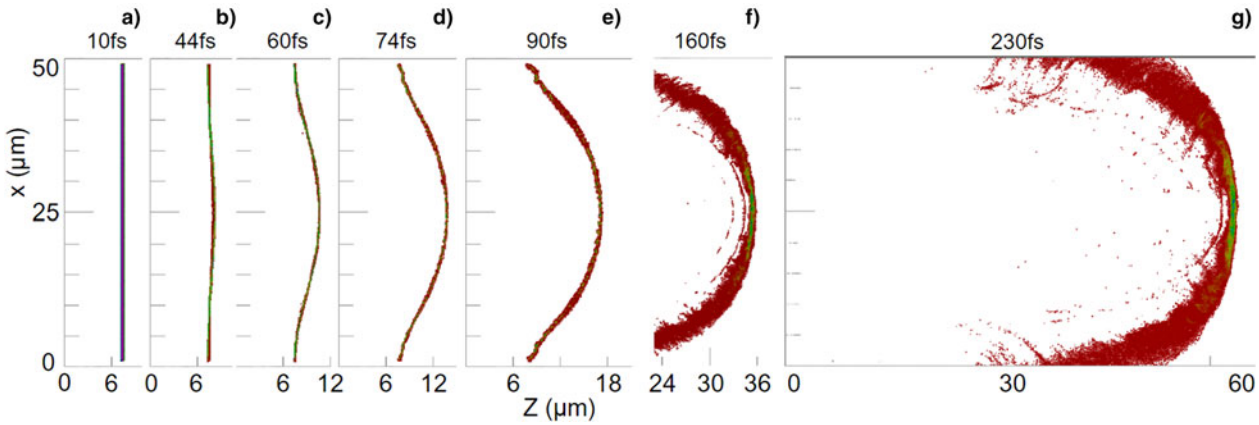

Fig. 2. Ion density n_i/n_c in flat target case at (a) 10, (b) 44, (c) 60, (d) 74, (e) 90, (f) 160, and (g) 230 fs.

https://doi.org/10.1017/S0263034615000026 Published online by Cambridge University Press

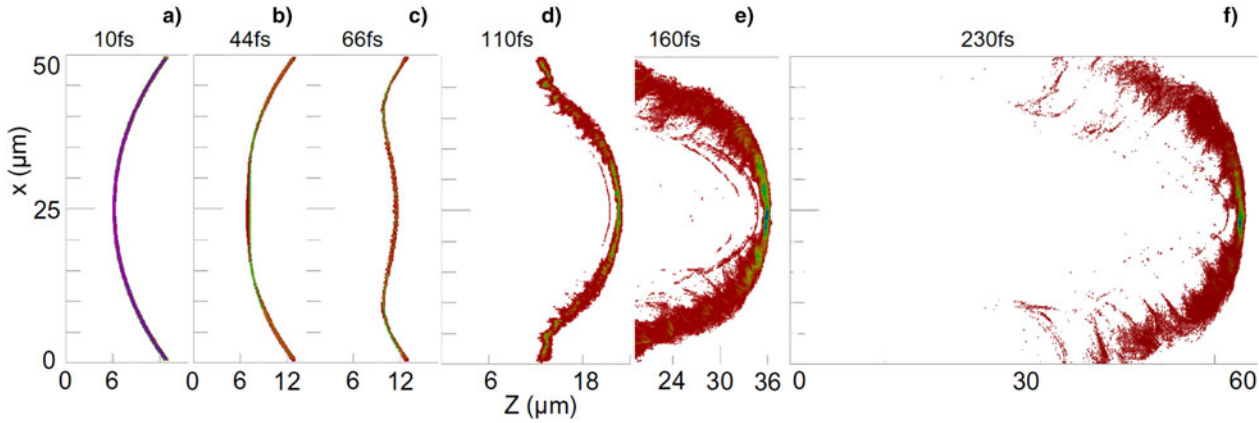

Fig. 3. Ion density n_i/n_c in convex target case at (a) 10, (b) 44, (**c**) 66, (d) 110, (**e**) 160, and (f) 230 fs. Target radius of the curvature is 50 μm.

continues to work as a relativistic plasma mirror for laser. Figure 2g shows the foil at the end of simulation, having peak density of accelerated bunch at 52 n_c. The curvature of the foil within the laser spot size has not changed from Figure 2e to 2g, but the thickness has increased, suggesting a slight increase in the energy spread of the accelerated bunch.

Ion density n_i/n_c in the convex target case is plotted in Figure 3 at (a) 10, (b) 44, (c) 66, (d) 110, (e) 160, and (f) 230 fs. Convex foil of 50 μm radius of the curvature, before laser irradiation is shown in Figure 3a. After the hole-boring stage two layers start to appear in Fig. 3b. Shape-changing phase of the foil due to Gaussian laser pulse is shown in Figure 3c, where the transverse bunching of protons has also appeared. The foil attains its final shape and looks like a concave foil in Figure 3d. After this stage, the foil is accelerated by the laser pulse and the final foil shape at the end of simulation is shown in Figure 3g. Density of the accelerated bunch is 45 n_c. In initial stages of the acceleration process, the geometrical effect in the convex target slightly enhances the number of protons in the detached foil. This happens because protons come out in the normal direction from the convex foil after the hole-boring stage and gets focused. This effect can be observed in the proton phase space plot in the (z, x) plane in Figure 4 at (a) 10, (b) 44, and (c) 60 fs. The focusing of protons ejected normally from the foil during the formation of detached layer is shown in Figure 4b and 4c. This results in more number of protons in the detached foil, but energy spread is higher. It happens due to comparatively longer shape change phase in convex targets as compared with the flat target case.

Ion density n_i/n_c in the concave target case at (a) 10, (b) 28, (c) 38, (d) 55, (e) 110, (f) 160, and (g) 230 fs. Target radius of the curvature is 50 μm. Figure 5b and 5c shows compressed foil in the hole-boring stage. Transverse bunching is lowest in Figure 5d as foil is not changing its shape. This becomes possible because the radius of curvature of the foil is chosen after simulating the flat target case, and the estimated radius of curvature of the final curved foil in Figure 2e is 50 μm. Figure 5e–5g shows the detached foil as it is further accelerated to higher energies. Increment in foil thickness is very small and peak density of accelerated bunch is 60 n_c, the highest among all the three targets considered. The growth of transverse instabilities in initial stages is lowest due to the absence of the shape change phase. Geometrical effects responsible for slightly more number of protons in the case of convex target are reversed and the total amount of accelerated charge is the lowest. The benefits of concave target become more clear from the energy spectra of protons plotted in Figure 6 for all the three target cases. Due to more stability in the concave case, accelerated proton beam has a peak energy around 3.2 GeV as compared with the peak energies of flat and convex targets found to be around 3.0 and 2.8 GeV, respectively. Total accelerated charge and energy spread are highest in convex followed by flat and concave targets.

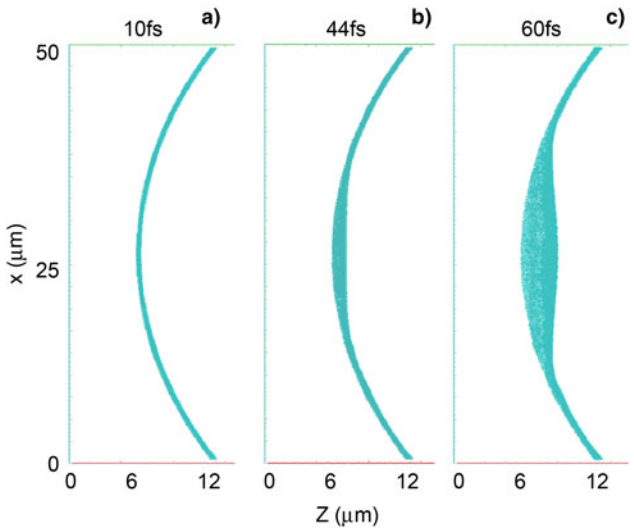

Fig. 4. Ion phase space in the (z, x) plane at (a) 10, (b) 44, and (c) 66 fs, for the convex target case.

https://doi.org/10.1017/S0263034615000026 Published online by Cambridge University Press

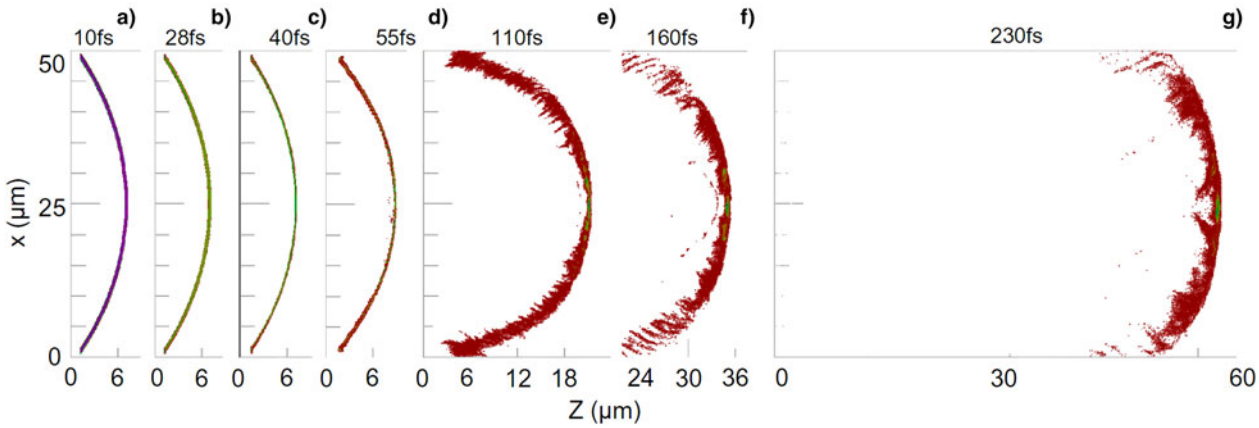

Fig. 5. Ion density n_i/n_c in concave target case at (a) 10, (b) 28, (c) 38, (d) 55, (e) 110, (f) 160, and (g) 230 fs. Target radius of curvature is 50 μm.

Equation (12) is numerically evaluated for the characteristic parameters described in the simulation section and results are plotted in Figure 7. For laser of spot size 50 μm and equal radius of curvature of the convex foil, it is observed to reverse the curvature after propagating to ∼40 μm (Fig. 7c). For short spot sizes 25 and 10 μm of the pulse, the foil becomes flattened after traversing the normalized distance ∼0.35 and ∼0.50 r_0, respectively (Fig. 7a and 7b).

In conclusion, the curvature in target affects the energy spread, peak energy, and amount of charge accelerated in the RPA regime. During the shape-changing phase of the acceleration process, target shapes modifies the growth of transverse instabilities, geometrical effects responsible for stability, and the total amount of charge accelerated in ion acceleration process. If the radius of curvature of concave target is chosen such that no change in shape occurs during the laser irradiation then acceleration process becomes much more stable leading to less energy spread and higher peak energy. The ratio of pulse spot size to the radius of curvature is a crucial parameter for obtaining the optimized change in foil curvature as it accelerates. The conjecture is validated by the numerical estimates and simulation results. One may envisage other types of target structuring such as rippling or non-uniformity based on the above model for efficient ion acceleration schemes.

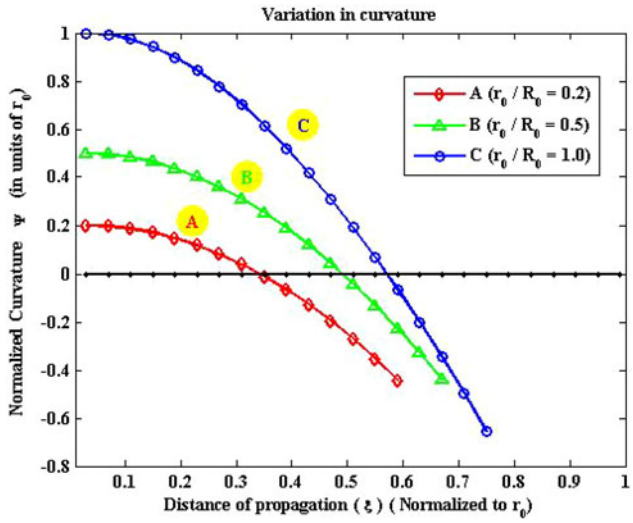

Fig. 7. The normalized variation in the curvature of the foil as the center of the foil propagates with respect to the normalized distance. The initial radius of curvature to the laser spot size ratio is 0.2, 0.5, and 1.0 in plot (A), (B), and (C), respectively.

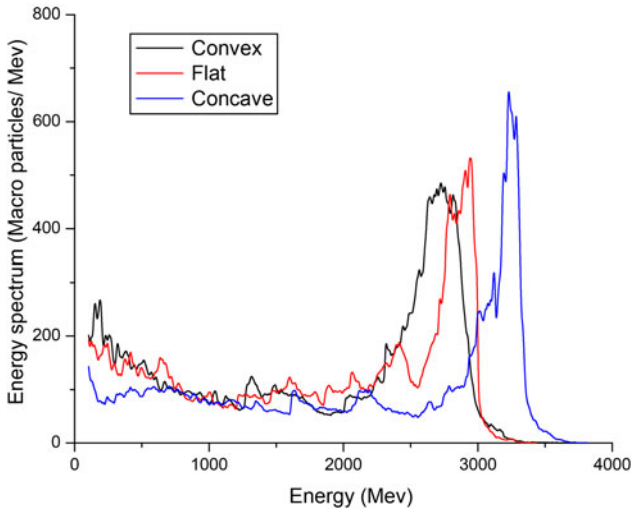

Fig. 6. Energy spectra of ions in region of $z > 20$ μm and 10 μm$< x >$ 40 μm at $t = 230$ fs for all the three target cases.

ACKNOWLEDGEMENTS

The work was carried out under the financial support from DST, Govt. of India.

REFERENCES

Ahmad, R., Rafique, M.S., Tahir, M.B. & Malik, H. (2014). Implantation of various energy metallic ions on al substrate using

https://doi.org/10.1017/S0263034615000026 Published online by Cambridge University Press

a table top laser driven ion source. *Laser Part. Beams* **32**, 261–270.

Akram, M., Bashir, S., Hayat, A., Mahmood, K., Ahmad, R. & Khaleeq-U-rahaman, M. (2014). Effect of laser irradiance on the surface morphology and laser induced plasma parameters of zinc. *Laser Part. Beams* **32**, 119–128.

Andreev, A., Platonov, K. & Kawata, S. (2009). Ion acceleration by short high intensity laser pulse in small target sets. *Laser Part. Beams* **27**, 449–457.

Bagchi, S., Kiran, P.P. & Bhuyan, M.K. (2008). Hotter electrons and ions from nano-structured surfaces. *Laser Part. Beams* **26**, 259264.

Bin, J.H. (2009). Influence of the target front-surface curvature on proton acceleration in laser-foil interaction. *Phys. Plasmas* **16**, 043109.

Borghesi, M. (2004). Multi-MeV proton source investigations in ultraintense laser-foil interactions. *Phys. Rev. Lett.* **92**, 055003.

Borghesi, M., Campbell, D.H., Schiavi, A., Haines, M.G. & Willi, O. (2002). Electric field detection in laser-plasma interaction experiments via the proton imaging technique. *Phys. Plasmas* **9**, 2214.

Brady, C.S. & Arber, T.D. (2011). Rayleigh-Taylor instability of an ultrathin foil accelerated by the radiation pressure of an intense laser. *Plasma Phys. Control. Fusion* **53**, 015001.

Bulanov, S.V., Esirkepov, T.Z., Khoroshkov, V.S., Kuznetsov, A.V. & Pegoraro, F. (2002). Oncological hadrontherapy with laser ion accelerators. *Phys. Lett. A* **299**, 240.

Chen, M., Pukhov, A., Sheng, Z.M. & Yan, X.Q. (2008). Laser mode effects on the ion acceleration during circularly polarized laser pulse interaction with foil targets. *Phys. Plasmas* **15**, 113103.

Clark, E. (2000). Measurements of energetic proton transport through magnetized plasma from intense laser interactions with solids. *Phys. Rev. Lett.* **84**, 670.

Eliasson, B., Liu, C.S., Shao, X., Sagdeev, R.Z. & Shukla, P.K. (2009). Laser acceleration of monoenergetic protons via a double layer emerging from an ultra-thin foil. *New J. Phys.* **11**, 073006.

Fourkal, E., Velchev, I., Fan, J., Luo, W. & Maet, C.M. (2007). Energy optimization procedure for treatment planning with laser-accelerated protons. *Med. Phys.* **34**, 577.

Gibbon, P. (2005). Resistively enhanced proton acceleration via high-intensity laser interactions with cold foil targets. *Phys. Rev. E* **72**, 026411.

Hegelich, B.M., Albright, B.J., Cobble, J., Flippo, K., Letzring, S., Paffett, M., Ruhl, H., Schreiber, J., Schulze, R.K. & Fernandez, J.C. (2006). Laser acceleration of quasi-monoenergetic MeV ion beams. *Nature* **439**, 441–444.

Jablonski, S., Badziak, S. & Raczka, P. (2014). Generation of high-energy ion bunches via laser-induced cavity pressure acceleration at ultra-high laser intensities. *Laser Part. Beams* **32**, 129–135.

Jain, V., Maheshwari, K.P., Jaiman, N.K. & Malav, H. (2013). Non-linear interaction of ultra-intense ultra-short laser pulse with a relativistic flying double-sided dense plasma slab/mirror. *Laser Part. Beams* **32**, 253–260.

Kim, I.J., Pae, K.H., Kim, C.M., Kim, H.T., Sung, J.H., Lee, S.K., Yu, T.J., Choi, I.W., Lee, C.L., Nam, K.H., Nickles, P.V., Jeong, T.M. & Lee, J. (2013). Transition of proton energy scaling using an ultrathin target irradiated by linearly polarized femtosecond laser pulses. *Phys. Rev. Lett.* **111**, 165003.

Kumar, M., Singh, R. & Verma, U. (2014). Bremsstrahlung soft X-ray emission from clusters heated by a Gaussian laser beam. *Laser Part. Beams* **32**, 9–14.

Lee, H.J., Pae, K.H., Suk, H. & Hahn, S.J. (2004). Enhancement of high-energy ion generation by preplasmas in the interaction of an intense laser pulse with overdense plasmas. *Phys. Plasmas* **11**, 1726.

Macchi, A., Cattani, F., Liseykina, T.V. & Cornolti, F. (2005). Laser acceleration of ion bunches at the front surface of overdense plasmas. *Phys. Rev. Lett.* **94**, 165003.

Macchi, A., Sgattoni, A., Sinigardi, S., Borghesi, M. & Passoni, M. (2013). Advanced strategies for ion acceleration using high power lasers. *Plasma Phys. Contr. Fusion* **55**, 124020.

Macchi, A., Veghini, S. & Pegoraro, F. (2009). Light sail acceleration reexamined. *Phys. Rev. Lett.* **103**, 085003.

Nieter, C. & Cary, J.R. (2004). VORPAL: a versatile plasma simulation code. *J. Comput. Phys.* **196**, 448.

Palmer, C.A.J., Schreiber, J., Nagel, S.R., Dover, N.P., Bellei, C., Beg, F.N., Bott, S., Clarke, R.J., Dangor, A.E., Hassan, S.M., Hilz, P., Jung, D., Kneip, S., Mangles, S.P.D., Lancaster, K.L., Rehman, A., Robinson, A.P.L., Spindloe, C., Szerypo, J., Tatarakis, M., Yeung, M., Zepf, M. & Najmudin, Z. (2012). *Phys. Rev. Lett.* **108**, 225002.

Patel, P. (2003). Isochoric heating of solid-density matter with an ultrafast proton beam. *Phys. Rev. Lett.* **91**, 125004.

Pegoraro, F. & Bulanov, S.V. (2007). Photon bubbles and ion acceleration in plasma dominated by the radiation pressure of an electromagnetic pulse. *Phys. Rev. Lett.* **99**, 065002.

Psikal, J., Tikhonchuk, V.T., Limpouch, J., Andreev, A.A. & Brantov, A.V. (2008). Ion acceleration by femtosecond laser pulses in small multispecies targets. *Phys. Plasmas* **15**, 053102.

Qiao, B., Zepf, M., Borghesi, M. & Geissler, M. (2009). Stable GeV ion-beam acceleration from thin foils by circularly polarized laser pulses. *Phys. Rev. Lett.* **102**, 145002.

Regam, C. (2011). Cone-guided fast ignition with ponderomotively accelerated carbon ions. *Plasma Phys. Control. Fusion* **53**, 045014.

Robinson, A.P.L., Gibbon, P., Zepf, M., Kar, S., Evans, R.G. & Bellei, C. (2009). Relativistically correct hole-boring and ion acceleration by circularly polarized laser pulses. *Plasma Phys. Control. Fusion* **51**, 024004.

Roth, M. (2001). Fast ignition by intense laser-accelerated proton beams. *Phys. Rev. Lett.* **86**, 436.

Sentoku, Y., Mima, K., Ruhl, H., Toyama, Y., Kodama, R. & Cowan, T.E. (2004). Laser light and hot electron micro focusing using a conical target. *Phys. Plasmas* **11**, 3083.

Shoucri, M., Afeyan, B. & Lefort, M.C. (2008). Numerical simulation for ion acceleration in an intense laser wave incident on overdense plasma. *J. Phys. D: Appl. Phys.* **41**, 215205.

Silva, L.O., Fonseca, R.A., Tonge, J.W., Mori, W.B. & Dawson, J.M. (2002). On the role of the purely transverse Weibel instability in fast ignitor scenarios. *Phys. Plasmas* **9**, 2458.

Spencer, I., Ledingham, K.W.D., Singhal, R.P., Mccanny, T., Mckenna, P., Clark, E.L., Krushelnick, K., Zepf, M., Beg, F.N., Tatarakis, M., Dangor, A.E., Norreys, P.A., Clarke, R.J., Allott, R.M. & Ross, I.N. (2001). Laser generation of proton beams for the production of short-lived positron emitting radioisotopes. *Nucl. Inst. Methods Phys. Res. B* **183**, 449.

Temporal, M., Ramis, R., Honrubia, J.J. & Atzeni, S. (2009). Fast ignitions induced by shocks generated by laser-accelerated proton beams. *Plasma Phys. Control. Fusion* **51**, 035010.

https://doi.org/10.1017/S0263034615000026 Published online by Cambridge University Press

Tripathi, V.K., Liu, C.S., Shao, X., Eliasson, B. & Sagdeev, R.Z. (2009). Laser acceleration of monoenergetic protons in a self-organized double layer from thin foil. *Plasma Phys. Control. Fusion* **51**, 024014.

Trtica, M., Batani, D., Redaelli, R., Limpouch, J., Kmetik, V., Ciganovic, J., Stasic, J., Gakovic, B. & MOMCILOVIC, M. (2013). Titanium surface modification using femtosecond laser with 10131015 W/cm^2 intensity in vacuum. *Laser Part. Beams* **31**, 2936.

Yan, X.Q., Chen, M., Sheng, Z.M. & Chen, J.E. (2009). Self-induced magnetic focusing of proton beams by Weibel-like instability in the laser foil-plasma interactions. *Phys. Plasmas* **16**, 044501.

https://doi.org/10.1017/S0263034615000026 Published online by Cambridge University Press